

# Structural health monitoring of concrete arch dams using the wavelet transform and modal assurance criterion methods

Amir Meysam Giahi<sup>1</sup>, Jafar Asgari Marnani<sup>2\*</sup>, Mohammad Sadegh Rohanimanesh<sup>3</sup>,  
Hassan Ahmadi<sup>4</sup>

<sup>1,2,3</sup> *Department of Civil Engineering, Faculty of Civil and Earth Resources Engineering, Central Tehran Branch, Islamic Azad University, Tehran, Iran.*

<sup>4</sup> *Department of Civil Engineering, Roudehen Branch, Islamic Azad University, Tehran, Iran*

*\*Corresponding author, E-mail: j\_asgari@iauctb.ac.ir; 00989193124871*

**Abstract.** Structural health monitoring of dams is a necessary issue in water supply network. Not identifying the local damages in these super structures and their extension could lead to abrupt and total collapse and impose major life or financial losses. This research investigates the effects of damage on the concrete arch dams and the methods for their detection. For this purpose the finite element model of a concrete arch dam was analyzed using the wavelet transform once by static frequency analysis and the second time when it is subjected to dynamic accelerograms. In the wavelet transform method using the static frequency analysis, cracks were formed on the dam body and the obtained results were compared to those obtained from Modal Assurance Criterion (MAC) method. In the wavelet transform method, by applying dynamic loads, different damage scenarios, including 16 damage locations and 3 damage levels (change in the materials properties) were compared to the healthy state of the dam. In order to process the wavelet transforms the displacements obtained from the modal and dynamic analyses were utilized. The results showed that employing wavelet transform method by applying dynamic loads could better detect the damages.

**Keywords:** damage detection, concrete arch dam, wavelet transform, frequency domain, modal assurance criterion

## 1. Introduction

Structural health monitoring (SHM) has been the subject of many researches in recent years, the general purpose of the mentioned methods is to obtain an accurate assessment of the current conditions of the structure at any moment of the operation, so that the correct decision can be made regarding the reconstruction and maintenance of the structure. These methods are usually based on collecting information obtained from the behavior of the structure and any changes in the response of the structure as a result of changes in environmental conditions, temperature, displacement, velocity, stress, strain, stress and curvature. Therefore, safety and optimal design of dams are necessary both in terms of designing new dams and health monitoring of old ones [1-4]. Among the various types of concrete dams, the arch dams are good options both in economic terms and reliability for harness of surface waters.

Structural damage detection using the vibration-based methods, due to their non-destructive nature, are under focus of attention. The importance of this issue is doubled for concrete arch dams. Not detecting local damages in these superstructures and their extension could lead to total and abrupt collapse and consequently impose major life and financial losses at the national and global levels. Structural health monitoring is a process for obtaining precise momentary information on the structural performance and conditions [5]. The main goal of the monitoring is detection of unusual behavior of the structure which indicates the undesirable structural conditions. In the topic of structural health monitoring, damage means changes that occur during service life of the structure and damage detection includes all the methods and techniques which diagnose damage and determine its amount [6-8]. In [9] studied a system-identification damage detection technique for concrete dams employing the extended coupled finite element-wavelet transform. The goal of the current research is to develop a method for detecting seismic cracking of concrete dams by coupling of extended FEM according to the cohesive cracks portions (XFEM-COH) and continuous wavelet transform (CWT). First, using the traditional FEM, the dam is numerically modelled. Then, by using XFEM-COH to the concrete dams, the cracking capability is considered in the dam. The outcomes of techniques under seismic excitations are compared and identified for the aims of damage detection. While in some structural health monitoring techniques there are some predefined damages, but the advantage of XFEM model lies in the fact that the entire structure of the dam without initial cracking is potentially susceptible to damage hazard but it may not experience cracking. Ultimately, to investigate any changes in the system, i.e. determining

probable impacts of cracking and nonlinear behavior, their corresponding modal parameter and changes are investigated using a detection system based on CWT. The findings show that the extended FEM-wavelet transform has a high capability for online SHM of concrete dams. By analyzing the results of damaged dam and obtaining the output of physical changes history, one could determine the initiation time of cracking and accurate location of damage by comparing to the results of healthy dam. The modal FEM and damaged XFEM parameters of dam response are among the important parameters in damage detection. Furthermore, any small change in the system is considerable [10]. In [11] performed a research on damage detection in the irregular plates and regular dams using combined wavelet transform-ANFIS method. This article presents a technique for damage detection for irregular and regular plates based on combination of wavelet transform and ANFIS methods. Most of damage specifying approaches required the structure responses before and after damage occurrence. But the present approach only needs structure response after the damage. While most of previous approaches only investigate damage of regular plates but the present method could investigate damage in the irregular plate, too. In the initial step the structure (irregular plate or regular dam) is designed in the ANSYS and analyzed and the damaged structure responses are calculated using the finite element approach. At the second stage, the responses are calculated at the finite element nodes with regular distances using ANFIS. The damage part is marked with decreased elasticity modules. Then these structure responses are investigated using 2D wavelet transform. It is demonstrated that the coefficients matrices of 2D wavelet transform could detect damages of regular plates and dams by disturbance in the damaged zone [12].

In [13] investigated the wavelet-transform-based higher order statistics for damage detection in rolling-element bearings. Signal processing has a vital role in diagnosing faults in mechanical systems. A method, i.e. the wavelet-transform-based higher order statistics was proposed in this article to detect fault in rolling-element bearings. The WTK diagrams of vibration signals gained of bearings with severe damages and different locations for detection and classification of damage were determined. The results revealed the excellent capability of WTK in processing vibration signals and defect diagnosis [14]. In [15] carried out a research on the time-frequency used for structural health monitoring. They included dam damages in a retaining one (Germany), strange behavior of the installed sensors in a levee located in Boston (UK) and a levee on Rhine (Germany).

In [16] studied the proper installment of sensors on a concrete dam utilizing a Quantum Genetic Algorithm. Their goal was identifying the modal parameters of the structure. For this purpose, they presented an effective and independent (EFI) criterion using the modal strain energy (MSE) and thus they could determine the optimal sensor placement on the upstream face of high concrete arch dams. In [17] proposed a hybrid method for optimal placement of sensors to monitor dynamic response of hydro-structures. They combined the MAC method with modal strain energy method and thus introduced a new one to reduce the effect of initial position of sensors. In this research, simulation was done on an arch dam considering 20 sensors and the first six orders of modal variations. Also in this article the advantages and disadvantages of the proposed method in comparison with such methods as MAC, modal kinetic energy criterion, Fisher information matrix and root-mean square error criterion were investigated. In [18] studied a concrete gravity dam. In their research they used MAC method to determine the damage location on the concrete gravity dam by implementing Hilbert-Hung method. The findings showed that based on the proposed criterion one could determine the correct length and position of damage on the concrete gravity dam.

In [19] selected a concrete dam for the case study and varied the structure of material types and construction, different models of the integrated dam were proposed. Then the elasto plastic analysis of dam-reservoir was performed for six different schemes. Finally through a comparative study, an optimal model of the integrated dam design was identified and presented. In [20] performed extensive studies on the damage location of a concrete dam. They concluded that the seismic damage detection system not only could be used for seismic damage process monitoring by measuring the dynamic stress history, but it could be utilized for detecting damage distribution in the defected region of the dam. In [21] presented an approach for monitoring damage in irregular 2D and 3D continuum structures according to the combined wavelet transform method. They used neural network model and based on the displacement and stress output values obtained from the damaged structure analysis, detected the damage location in the structure. In the

presented method for damage detection, the responses obtained from analyses that were performed before and after the damage were investigated. Their method proved that has a high efficiency in detecting the damage location on the structure. In [8] presented an optimization method using the Fisher Information Matrix Firefly Algorithm (FIMFA). In the proposed method, the optimized sensors were very effective in detecting damages especially for large and complex structures. They showed that the FIMFA method has the potential to be extended to a wide range of SHM uages in complicated structures.

Overall, a general review of the performed research on damage detection reveals that the investigated systems were mostly comprised of simple structural elements such as frames, beams or trusses (which had much simpler governing equations than those that correspond to the behavior of a dam). The reason that concrete arch dams have less been studied lies in the fact that they become complicated in modeling, analysis and during considering interactions between different environments. Also presence of higher degrees of freedom in dams compared to other types of structures is another reason for being complicated problems and green energy management [22-25].

Due to the size and dimensions of the dam, its investigation procedure is complicated. In this study, an attempt has been made to investigate and identify the location of damage using the simplest analytical tools. The main conterbiution is comparing dynamic and static analysis methods in identifying the location of damage, to evalute the method accuracy and efficacy according to the location of damage. In addition, compared to previous works, in this paper, Assurance Criterion (MAC) method [26] is used to determine the optimal sensor installation location, which has better performance. For this purpose, first the concrete arch dam together with the fluid behind it (water) is modeled and meshed using the ABAQUS software for the case that the dam is filled up to its top. Then in the MATLAB software using the wavelet transform code, damage detection on dam body is performed for the two states of damaged and healthy dams by considering the static and dynamic analyses and employing MAC method.

## **2. Materials and methods**

### *2.1 Damage detection using the Modal MAC method*

MAC is a broadly employed tool for quantitative comparison of modal vectors. The aim of using this criterion is depicting relationship between two sets of mode shapes. Also this criterion is applied for evaluating and comparing between the experimental and analytical modal vectors. The MAC is calculated as the normalized scalar product of two sets of vectors  $\{\phi_A\}$  and  $\{\phi_B\}$  [27].

A zero value for MAC shows lack of consistency and a value equal to unity shows the consistency relation. The MAC matrix is formed considering all modal vectors  $i$  and  $j$  from the two sets of mode shapes, so that dimensions of this matrix is dependent on the number of considered mode shapes.

In the damage monitoring method employing MAC, one could detect damages in terms of stiffness through investigating the differences between changes in the natural frequencies and displacements of the healthy and damaged dams. Furthermore, investigating damage at different locations and examining the results using statistical methods one could also detect the damage location. Therefore, detecting changes in the natural frequencies and mode shapes are among the main parameters employed for damage detection.

### *2.2 Wavelet transform*

There is a procedure of math models which are utilized for decomposing a signal, continuously into its frequency components so that the resolution of per part is deponds on its scale. A wavelet transform is in fact decomposition of a function according to the wavelet functions. Wavelets are transmitted and scaled piecman of a function with finite length, and highly damping oscillation.

#### *2.2.1 Mathematical definition of wavelet transform*

Wavelet transform is a function with two important features; it is oscillatory and short time.  $\Psi(\omega)$  is a wavelet function, if and only if its Fourier transform into  $\Psi(\omega)$  could satisfy the condition of Equation (1):

$$\int_{-\infty}^{+\infty} \frac{|\Psi(\omega)|}{|\omega|^2} d\omega < +\infty \quad (1)$$

This status is defined as the admissibility status for  $\Psi(x)$  wavelet. The equation (1) could be regarded equivalent to the below formula (in other words, in order that the wavelet have the above condition, Equation (2) should be satisfied) [28]:

$$\int_{-\infty}^{+\infty} \Psi(x) dx = 0 \quad (2)$$

This type of the function with zero mean is not too restricting and one could find many functions which could be called wavelet function on that basis.  $\Psi(x)$  is the mother wavelet function and the functions utilized for dam vibration should be calculated so that having the coefficients, the structure damping could be determined according to the Rayleigh damping coefficients, which is also called frequency-based damping. The system damping is obtained by a linear combination of mass matrix and stiffness matrix using Equation (3). The parameters of this linear combination were calculated from the dam modal frequencies.

$$C = \alpha M + \beta K \quad (3)$$

$\alpha$  And  $\beta$  are the coefficients of Rayleigh linear combination calculated from Equations (4) and (5):

$$\alpha = \frac{2\xi\omega_i\omega_j}{(\omega_i + \omega_j)} \quad (4)$$

$$\beta = \frac{2\xi}{(\omega_i + \omega_j)} \quad (5)$$

In the equations 5, 6,  $\xi$  denotes damping ratio where in the frequency analysis  $\omega_i$  and  $\omega_j$  are taken equal to 5%.  $\omega_i$  and  $\omega_j$  are the angular frequencies of two modes of vibration. In analysis of Karun1 Dam, the Rayleigh damping factor are calculated from the first and third frequencies of vibration modes of the dam:  $\alpha = 0.1149$  and  $\beta = 0.0206$  and the critical damping ratio is calculated equal to 5%. Having the frequency values, the damping factors of the dam which are required for dynamic analysis were calculated. In this state, the dam is modelled without abutments and the boundary conditions are applied by preventing movement at the abutment nodes.

### 2.2.2 Continuous wavelet transform

Continuous wavelet transform is a type of transformation which translates a continuous function in time to the time-frequency space. The basis functions of the new space are wavelet functions. In mathematics, the continuous wavelet function of a continuous function  $x(t)$  is a square-integrable function defined for a scale parameter  $a > 0$  and position  $b \in \mathbb{R}$  as shown below [29]:

$$X_\omega(a, b) = \frac{1}{\sqrt{a}} \int_{-\infty}^{+\infty} x(t) \Psi^*\left(\frac{t-b}{a}\right) dt \quad (6)$$

Where,  $\Psi(t)$  is a continuous function in time and frequency, and is known as the mother wavelet.

### 2.2.3 Discrete wavelet transform

In the 1D discrete wavelet transform, the input signal  $s_0(n)$ , is decomposed into two portions of approximation coefficients and detail coefficients:

$$S_{i+1}(n) = \sum_{k=0}^{L-1} g(k)s_i(2n-k) \quad (7)$$

$$W_{i+1}(n) = \sum_{k=0}^{L-1} h(k)s_i(2n-k) \quad (8)$$

In the above equations  $g(k)$  and  $h(k)$  are the low and high pass filter factors, respectively and  $L$  is the filter size

#### 2.2.4 Graphic window of stationary wavelet window

The set of frequencies which are executed in a short period of signal could be equal to the set of frequencies in another time. This signal type is called a stationary signal. The SWT window is shown in Fig.1 and considering that figure the following could be identified:

- 1-Input signal
- 2-Signal without disturbance (perturbation)
- 3-Signal with disturbance only
- 4-Disturbed and decomposed signal
- 5- Non-disturbed and decomposed signal

Note: the index corresponding to decomposed signals (d1, d2) refers to the number of selected class.

The wavelet transform Daubechies (db2) is used with scale 2. In this section, the mode shape of the dam is shown at the left side and the transformed one by applying wavelet transform and using db2 method with scale 2 is shown at the right side. The d1 and d2 functions corresponding to the initial mode and transformed mode are also shown in the figure. As is seen, after applying the transform, the d1 and d2 functions have become zero and their noise is removed.

### 3. Studied model

A double-curvature concrete arch dam is considered for building the FEM and analysis of the investigated method. In this respect, Fig.1 shows two views from the top and side of this double-curvature concrete arch dam.

Fig.1 Geometry of the considered model for the double-curvature concrete arch dam, Plan and side view

Mechanical properties of the concrete materials used in construction of this dam are given in Table (1).

Table 1 Mechanical properties of the used materials in the dam

According to the material library in the Abaqus software, the mass of the material, which is one of the most important parameters in the modal, should be defined and then applied to the structure. Therefore, based on specific weight, the mass of concrete is determined and applied to the structure. In this study, the behavior of concrete materials is defined based on the concrete failure index to consider the effect of nonlinear behavior. Also, the effects of small changes (non-linear effects) have been applied in the modeling by activating the NLgeom option in the Abaqus software.

For modelling by the finite element method in ABAQUS software, the 3D 8-node brick element C3D8R is used. Also for integration the 8-node Gauss method is employed. In order to determine the modal characteristics of the healthy structure, based on the assumptions presented in the previous section, first a modal linear analysis is performed in the ABAQUS software. As mentioned before, it is not possible to consider all the vibration modes in analysis of concrete arch dams due to very large number of degrees of freedom in these systems. Therefore the modes with greater effect on the vibration response of the structure should be determined using an appropriate method.

### 3.1 Validation

For validation of the model, the Hultgren's research work is used [30]. In this research a concrete arch dam with 220m height which is symmetric with double curvature is used for modelling. In this model, the crest length of dam is 430m and the length of dam span at the bottom is 80m. The width of dam crest is 8m and the dam thickness at the bottom is 55m. The dam height is equal to 220m. The properties of used materials in the dam are shown in Table (2).

In Table (3) a comparison is made between the results obtained from numerical modelling by the ABAQUS software and those of the selected article [30]. All the studies in this study were performed on a model of an arch dam with a foundation and associated reservoir provided by the ICOLD Benchmark Workshop [30]. This dam is a 220-meter-long symmetrical arch dam with a width of 430 meters at the top and 80 meters at the bottom. The thickness in the central part varies from 8 meters at the top to 55 meters at the base.

Table 2 Properties of the dam and water behind the studied dam [30]

Table 3 Frequency modes of the studied dam

The exerted loads on the structure include the weight of dam and hydrodynamic force applied by the water in the reservoir. The results obtained from modal analysis for the first ten modes are presented in Table (3) both for the present study and [30]. As is seen, the results obtained from both models are in good agreement.

The acoustic property of that material is used to model mechanical waves in gases, liquids and solids. In this article, the seismic acoustic properties of water under waves caused by seismic vibrations have been used to model water. The equation of water movement in a tank with limited flow can be written as follows:

$$\frac{\partial p}{\partial x} + \rho_f \ddot{u}^f = 0 \quad (9)$$

so that  $p$  is fluid pressure,  $\rho_f$  fluid density,  $x$  is specific position of fluid and  $\ddot{u}^f$  specific acceleration of fluid. Assuming a linear and compressible fluid, the pressure exerted by the fluid is expressed according to the following equation [31]:

$$p = -K_f \nabla u^f \quad (10)$$

$K_f$  is the bulk modulus of a liquid, which is calculated according to the density of the liquid and the speed of sound in the liquid,  $C_f$  is calculated from the following equation [32]:

$$K_f = \rho_f c_f^2 \quad (11)$$

By combining the last relations, the fluid acoustic equation is obtained according to the following relation.

$$\frac{1}{K_f} \ddot{p} - \frac{\partial}{\partial x} \left( \frac{1}{\rho_f} \frac{\partial p}{\partial x} \right) = 0 \quad (12)$$

In this study, in order to investigate the optimal location of the sensor on the concrete dam, the interaction of water and the dam structure is considered, and the soil effect is applied to the model in the form of a support condition by closing the translational degrees of freedom under the dam and the water.

### 3.2 Failure modelling

The points and elements used for the damage detection study are selected randomly. These points are shown in Fig.2

Fig.2 Different failure scenarios at different locations of the concrete arch dam

In order to perform the wavelet transform by the static method, use is made of cracks at the shown locations which are compared with the MAC damage detection method. But in the wavelet transform method using the dynamic method, assuming reduced stiffness and softening of system due to failure, damage is modeled as reduction in modulus of elasticity, E. In this respect the modulus of elasticity value is calculated for the three damage levels (including 10, 30 and 50%). The location of the studied points is shown in Table (4).

Table 4 Location of the selected points

After investigating of the dam utilizing the ABAQUS software, the response obtained from it is utilized for wavelet analysis in the MATLAB software and the special wavelet. The displacements were measured along transverse direction of the dam (U1) and longitudinal direction of the reservoir (U2) for the first vibration mode and 56 points in the healthy dam body with equal distances. This response is analyzed with a frequency equal to 1.88 Hz using the db2 wavelet (scale 2). Similarly, after modeling the dam and its failure using the ABAQUS software, the response of the cracked sample i.e. the displacements along transverse direction (U1) and along the reservoir direction (U2) for the first mode and 56 points at the dam crest were measured with equal distances. The response was analyzed using the MATLAB software in the special wavelet toolbox and application of Db2 wavelet.

#### 4. Results and discussion

In this section, by implementing modal analysis the obtained results are presented in Table (5), in the form of frequency values due to damage in different parts of the dam and with different severities.

Table 5 The values of the first ten frequencies of the structure due to damage in different areas of the dam

Now, using Equation (9), the relative frequency changes are calculated due to different failure severities at different parts of the dam.

$$e_f^i = \frac{f_{ud}^i - f_d^i}{f_{ud}^i} \quad (13)$$

Where,  $e_f^i$  denotes the relative frequency difference corresponding to the  $i$ th mode,  $f_{ud}^i$  denotes the natural frequency of the system without failure (in the healthy structure) in the  $i$ th mode and  $f_d^i$  denotes the natural frequency corresponding to the  $i$ th mode of the system with failure (in the damaged structure).

##### 4.1 Wavelet transform using the static analysis

In the static analysis, by creating crack at point 1 according to Fig.3, the modal analysis is performed on the dam.

Fig.3 Created crack at point 1 for performing modal analysis

Figs. 4 and 5 show the wavelet transform analyses along x direction for the healthy dam and damaged dam at point 1.

Fig.4 STW graph for the response of the healthy sample under the wavelet analyzer db2 (Model-U1)

Fig.5 STW graph for the response of the cracked sample under the wavelet analyzer db2 (Model-U1)

As is seen in Figs. 4 and 5, the diagrams include a significant jump at the crack location in the dam body, whereas in the healthy sample no disturbance or inconsistency is seen in the diagrams. In other words, as stated before, the crack location is assumed that is located at the middle of dam

crest at point 1. Also in practice and considering the figures, the location of disturbance is identical with the location of crack on the dam. The use of wavelet transform for detecting failure location is due to the SWT characteristics which distinguish it from other methods applied for damage detection. The wavelet transform has the property of variable resolution for different frequencies, whereas it presents the high frequency values and low frequency locations with lower resolution. This characteristic of SWT in terms of detecting damage location is desirable as crack causes change at high frequencies, and for detecting the damage location there is need for just detecting the location of these changes which is well accessible using SWT.

#### 4.2 Modal assurance criterion

Using Equation (10), the relative frequency changes are calculated at different parts of the dam due to different failure severities. Where  $e_f^i$  denotes the relative frequency difference corresponding to the  $i$ th mode,  $f_{ud}^i$  denotes the natural frequency of the system without failure (in the healthy structure) in the  $i$ th mode and  $f_d^i$  denotes the natural frequency corresponding to the  $i$ th mode of the system with failure (in the damaged structure).

In continuation, the relative frequency differences due to different failure severities at different parts of the dam body are calculated and the results are shown in table 6. In these figures, the horizontal axis indicates the number of structure modes and the vertical axis indicates percentage of frequency difference corresponding to each mode calculated by equation (10).

Table.6 Changes in the natural frequencies due to presence of failure with different severities at the top of the concrete arch dam

In the present research, 10 modes are considered, hence the MAC matrix is a 10x10 matrix. The more the diagonal elements of the MAC matrix approach unity and other elements approach zero, it means a higher logical consistency between two sets of responses.

In this study, the highest point located on the dam crest (point 1) is determined as the first optimal location for the first sensor by calculationg the values of MAC matrix. The second poit is obtained in a way that the greatest linear independence is established between mode shapes. In order to determine the second point, after determining the first point, the optimal value of the following matrix is calculated:

$$MAC(1, j) \quad j = 1, 2, \dots, n \quad (14)$$

In the above equation,  $n$  denotes the candidate points for the optimal location of sensors. After calculating the MAC matrix, the largest non diagonal element of each matrix should be calculated using the following equation:

$$\max\{Non - Diag[MAC(1, j)]\} \quad j = 1, 2, \dots, n \quad (15)$$

Finally the MAC matrix obtained from analysis of the results is shown in Fig.6.

Fig.6 MAC matrix along Z axis for the first 10 modes of point 5

As seen in Fig.6, for the first 10 modes at point 5 there is difference between frequencies of the healthy and damaged dams in all the studied modes of point 5. The points where their numerical value is unity are those that have a small difference but where this value approaches zero, it indicates that there is no consistency relation between the points. In modes no. 4, 6, 7, 8, 9 and 10 this difference is greater than other modes.

#### 4-3-Wavelet transform using dynamic analysis

For performing the wavelet analysis the Northridge Earthquake records are used. These records are shown in Fig.7

Fig.7 Accelerogram records of Northridge Earthquake

Observing Fig.8 it is seen that the failure is seen at the dam crest with maximum differences (in percentage) at points 1 and 5 between the healthy and damaged dam. Furthermore, it is observed that where the points approach the dam foundation the difference between the healthy and



damaged dams is reduced and sensitivity of damage is decreased. It is seen that at points 14 - 16 there is minimum difference between the healthy and damaged dams.

The points on the dam crest (a) , at quarter of the dam height (b), at middle of the dam height (c) and at three-quarter of the dam height (d) were selected as the studied points which are respectively named by letters a, b , c and d. The acceleration domain of these points are shown in Figs.9-13. Fig.9 show the studied points on the dam. Figures 10, 11 and 12 are depicted the difference between acceleration values corresponding to before and after 10, 30, and 50% failures respectively

Fig.8 Selected points on the model of studied dam used for dynamic wavelet transform

Fig.9 Difference between acceleration values corresponding to before and after 10% failure

Fig.10 Difference between acceleration values corresponding to before and after 30% failure

Fig.11 Difference between acceleration values corresponding to before and after 50% failure

Fig.12 Standard deviation of acceleration changes corresponding to different structural nodes for 10, 30 and 50% failure rates.

Figure 12 illustrates the Standard deviation of acceleration changes corresponding to different structural nodes for 10, 30 and 50% failure rates. Discrete-time Fourier transform for the discrete-time signal  $X[n]$  is defined as shown below [33]:

$$X(f) = \sum_{k=-Y}^Y x[n] \exp(-jk2\pi f) \quad (16)$$

The time and frequency domains variables are shown by  $n$  and  $f$ . The above equation which is formed from output function is in the frequency domain and includes the spectral characteristics of signal  $x[n]$  in the frequency domain. According to Fourier theorem, the behavior in the frequency domain of each function with finite domain  $a$  could be reconstructed as a linear combination of infinite sinusoidal parts with different domains, phases and frequencies. In this section, dam failure by earthquake vibrations in the frequency domain is investigated. For example, Fourier transform of time observations for a number of specimen nodes with and without failure are shown in Fig. 13.

Figure 13. Fourier transform of time observations for a number of specimen nodes with and without failure

The variance of between healthy and damaged nodes in lower nodes, is less than that of higher nodes (those located on the dam crest) which shows that the impact of earthquake on the dam crest is not related to damage location. In order to investigate the difference between undisturbed and damaged states, the difference between Fourier transform observations before and after 30% failure is shown in Fig.14

Fig.14 The difference between acceleration values before and after 30% failure in some of the nodes of sample

## 5. Conclusion

In this research damage detection on a concrete double-curvature arch dam is investigated. For this purpose the wavelet transform method was utilized by applying static analysis and dynamic accelerogram load. At first, the results of wavelet transform using static analysis were compared to those obtained from MAC. In the wavelet transform method using the static analysis method, the crack was applied to the dam body. In the wavelet transform method using the dynamic acceleration load, investigations were made for three levels of structural damage at different parts of the dam body.

Next, by defining two damage indices based on changes in the frequencies and using mode shapes for the first 10 vibration modes, the effect of damage on dynamic behavior of these systems was studied. Finally the dam displacements were studied at three sections of the middle, right corner and left corner of dam which were subjected to three levels of 10, 30 and 50% damages. Comparing the data obtained from the healthy dam and extracting the difference between the healthy dam and damaged dam data for three damage levels of 10, 30, and 50% (according to the wavelet transform in the MATLAB software), three relationships were derived. In General, the most important findings of this research could be summarized as follows:

- The excited vibration responses of the dam are not capable of detecting the damage location and one could only identify occurrence or not occurrence of large and severe damages using them.
- The vibration modes of the dam are appropriate responses for detecting damage in the dam and could simultaneously detect multiple damages.
- By increasing the height from the base of the dam by 25%, the probability of failure increases by 50%. This is despite the fact that with the increase of the distance, the behavior of the structure in two states of healthy and damaged are similar.
- Wavelet analysis as a novel and advanced tool for damage detection has a high capability in analysis of the structure vibration responses and could exhibit any type of discontinuity such as crack, decay and sudden reduction of stiffness in the form of disturbance or peak points.
- The acceleration at dam nodes is sensitive to existing damages. Albeit this sensitivity is just observable at adjacent nodes.
- In wavelet transform method, selection of an appropriate scale is highly effective on the detection accuracy and precision. In this study, through investigation it was found that a high scale is appropriate for detecting points with small damages and a low scale is appropriate for detecting points close to abutments.
- Dynamic wavelet analysis has a high accuracy and is capable of detecting damages in the dam structure even with very low percentage of damage in the dam elements.
- In the damage detection method using MAC, it was observed that while approaching the dam crest, the difference between frequencies of the healthy dam and damaged dam increases and this demonstrates that the points located on the dam crest are more sensitive to damage and their damage has greater impact on the frequency and modal behaviors of the dam
- In the wavelet transform method using static analysis, considering that both the area of elements is small and damage limited, the method could not detect the damage location by reducing stiffness of the structure. Hence, by applying cracks instead of reducing stiffness at the damage location, it was observed that locating cracks is also possible. Hence, for detecting crack location by the wavelet transform using static analysis, where the damage rate is small and its extent is limited we would encounter some problems. However we could detect damage location by the wavelet transform using static method only in case that stiffness is totally reduced.
- The wavelet transform using the dynamic accelerogram analysis demonstrate up to 98% accuracy and could detect any type of events and any type of reduction in elements. Therefore, this method has a much higher accuracy with respect to the wavelet transform method using the static analysis.

## References

1. Zhang, K., Lu, F., Peng, Y., et al., "A novel method for generation and prediction of crack propagation in gravity dams". *Structural Engineering and Mechanics*, **81**(6), 665-675, (2022).
2. Bouchaala, F., Ali, M. Y., Matsushima, J., et al., "Estimation of Seismic Wave Attenuation from 3D Seismic Data: A Case Study of OBC Data Acquired in an Offshore Oilfield". *Energies*, **15**(2), 534, (2022).
3. Assadi, A., & Najaf, H. "Nonlinear static bending of single-crystalline circular nanoplates with cubic material anisotropy". *Archive of Applied Mechanics*, **90**(4), 847-868, (2020).
4. Ali, W., Gohar, R., Chang, B. H., & et al., "Revisiting the impacts of globalization, renewable energy consumption, and economic growth on environmental quality in South Asia". *Advances in Decision Sciences*, **26**(3), 1-23, (2022).
5. Valente, N. A., Sarrafi, A., Mao, Z., & et al., "Streamlined particle filtering of phase-based magnified videos for quantified operational deflection shapes". *Mechanical Systems and Signal Processing*, **177**, 109233, (2022).

6. Tightiz L, & Yoo J. "Towards Latency Bypass and Scalability Maintain in Digital Substation Communication Domain with IEC 62439-3 Based Network Architecture". *Sensors*. 29;22(13):4916, (2022).
7. Kalenik, M., Wichowski, P., Chalecki, M., et al., "Efficiency of wastewater purification in medium sand with a lightweight expanded clay aggregate assisting layer". *Journal of Water and Land Development*, 57, 30-38, (2023).
8. Sharapov A., Arzamastsev A., Shatskikh Y., et al., "Improvement Of Heat Utilization Efficiency In Drying Plants", *Procedia Environmental Science, Engineering and Management*, **9** (1) 159-163, (2022).
9. Li, Q., Wang, G., Sarrafi, A., et al., "Dynamic Characteristics Identification of an Arch Dam Model via the Phase-Based Video Processing". *KSCE Journal of Civil Engineering*, **25**(1), 140-152, (2021).
10. Webber, J., Yano, K., Suga, N., et al. "WLAN Interference Identification Using a Convolutional Neural Network for Factory Environments", *J. Commun.*, **16**(7), 276-283, (2021).
11. Barbosh, M., Singh, P., & Sadhu, A. "Empirical mode decomposition and its variants: A review with applications in structural health monitoring". *Smart Materials and Structures*, **29**(9), 093001, (2020).
12. Alim A., Ngakan D., Naresh B., et al., "Multi Project Scheduling and Material Planning Using Lagrangian Relaxation Algorithm". *Industrial Engineering & Management Systems*, **20**(4), 580-587, DOI: 10.7232/IEMS.2021.20.4.580, (2021).
13. Lotfi, V., & Lotfi, A. "Time harmonic analysis of concrete arch dam-reservoir systems by utilizing GN high-order truncation condition". *Scientia Iranica*, In press, (2022).
14. Aslanova F. "A comparative study of the hardness and force analysis methods used in truss optimization with metaheuristic algorithms and under dynamic loading". *Journal of Research in Science, Engineering and Technology*. 29, 8(1), 25-33. DOI: <https://doi.org/10.24200/jrset.vol8iss1pp25-33>, (2022).
15. Chen, B., Huang, Z., Zheng, D., et al., "A hybrid method of optimal sensor placement for dynamic response monitoring of hydro-structures", **13**(5), 1550147717707728, (2017).
16. Esmailzadeh, S., Ahmadi, H. Hosseini, S. A. "Damage detection of concrete gravity dams using Hilbert-Huang method", *Journal of applied engineering sciences*, **8**(2), 7-16, (2018).
17. Shi, B. W., Li, M. C., Song, L. G., et al. "Deformation coordination analysis of CC-RCC combined dam structures under dynamic loads", *Water Science and Engineering*, **89**, 98-104, (2020).
18. Zhang, Y., Feng, X., Fan, Z., et al. "Experimental investigations on seismic damage monitoring of concrete dams using distributed lead zirconate titanate sensor network", *Advances in Structural Engineering*, 20(2), 170–179. <https://doi.org/10.1177/1369433216660002>, (2017).
19. Ghiasi, V., Heydari, F., & Behzadinezhad, H. "Numerical analysis and back calculation for embankment dam based on monitoring results (Case study: Iran-Lurestan Rudbar)", *Scientia Iranica*, **28**(5), 2519-2533, (2021).
20. Jalili H, Hosseinzade Dalir A, Farsadizadeh D., "Study of vortex flow extending around the reservoir sluice gate in order to increase in flushing efficiency", *Iranian Water Research Journal*, **15**, 51-62, (2014).
21. Zacchei, E., & Molina, J. L. "Application of artificial accelerograms to estimating damage to dams using failure criteria" *Scientia Iranica*, **27**(6), 2740-2751, (2020).
22. Matsushima, J., Ali, M. Y., Bouchaala, F. "Propagation of waves with a wide range of frequencies in digital core samples and dynamic strain anomaly detection: carbonate rock as a case study", *Geophysical Journal International*, **224**(1), 340-354, (2021).
23. Bouchaala, F., Ali, M. Y., Matsushima, J., et al. "Azimuthal investigation of compressional seismic-wave attenuation in a fractured reservoir". *Geophysics*, **84**(6), B437-B446, (2019).
24. Smagacz, J., & Martyniuk, S. "Soil properties and crop yields as influenced by the frequency of straw incorporation in a rape-wheat-triticale rotation". *Journal of Water and Land Development*, 56, 1-6, (2023).
25. Tightiz L, & Yoo J. A robust energy management system for Korean green islands project. *Scientific Reports*. 20;12(1):22005, (2022).
26. Liu, P., Chen, J., Fan, S., et al. "An improved system identification method for hardfill dams considering the spatial variability of material parameters based on random field theory", *Soil Dynamics and Earthquake Engineering*, **152**, 107067, (2020).
27. Bouchaala, F., Ali, M. Y., & Matsushima, J. "Compressional and shear wave attenuations from walkway VSP and sonic data in an offshore Abu Dhabi oilfield. Comptes Rendus". *Géoscience*, **353**(1), 337-354, (2021).
28. Assadi, A., Najaf, H., & Nazemizadeh, M. "Size-dependent vibration of single-crystalline rectangular nanoplates with cubic anisotropy considering surface stress and nonlocal elasticity effects", *Thin-Walled Structures*, **170**, 108518, (2022).
29. Nosoudi, A., Dabbagh, H., & Yazdani, A. "Performance-based reliability assessment of RC shear walls using stochastic FE analysis", *Structural Engineering and Mechanics*, **80**(6), 645-655, (2021).

30. Hellgren, R. "Influence of Fluid Structure Interaction on a Concrete Dam during Seismic Excitation:- Parametric analyses of an Arch Dam-Reservoir-Foundation system". (Dissertation). Retrieved from <http://urn.kb.se/resolve?urn=urn:nbn:se:kth:diva-145655> (2014).
31. Goldgruber, M., Shahriari, S., & Zenz, G. "Dynamic sliding analysis of a gravity dam with fluid-structure-foundation interaction using finite elements and Newmark's sliding block analysis", *Rock Mechanics and Rock Engineering*, **48**(6), 2405-2419, (2015).
32. Madina B, Gumilyov LN. "Determination of the Most Effective Location of Environmental Hardenings in Concrete Cooling Tower Under Far-Source Seismic Using Linear Spectral Dynamic Analysis Results". *Journal of Research in Science, Engineering and Technology*. **29**(1), 22-4. DOI: <https://doi.org/10.24200/jrset.vol8iss1pp22-24>, (2020).
33. Li, S., Wang, J. T., Jin, A. Y., et al. "Parametric analysis of SSI algorithm in modal identification of high arch dams", *Soil Dynamics and Earthquake Engineering*, **129**, 105929, (2020).

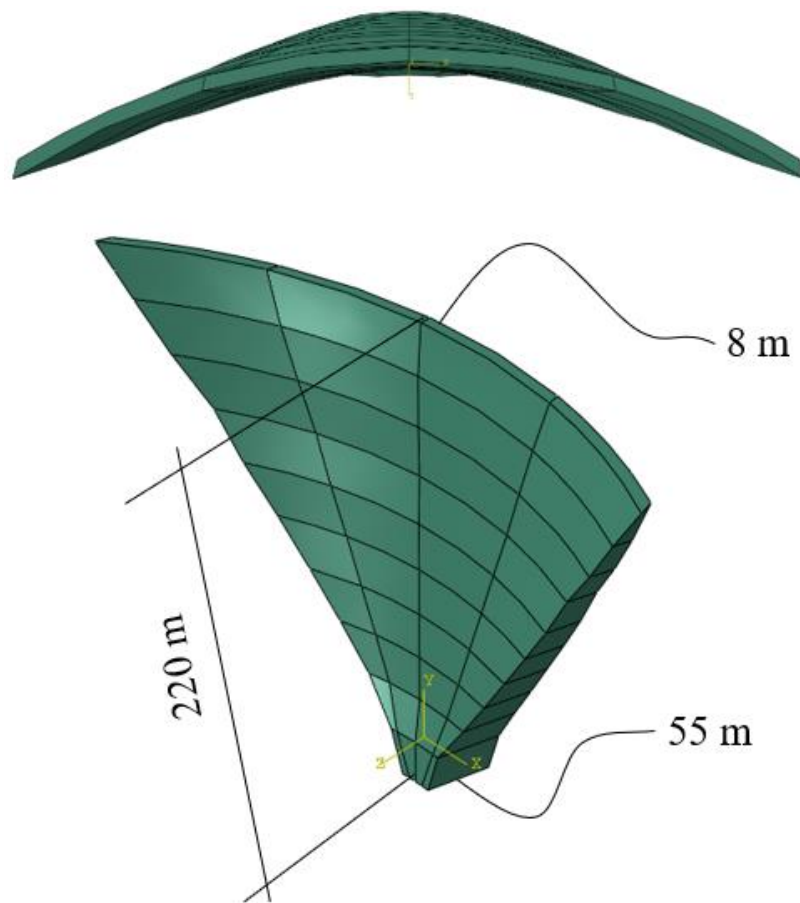


Fig.1 Geometry of the considered model for the double-curvature concrete arch dam, Plan and side view

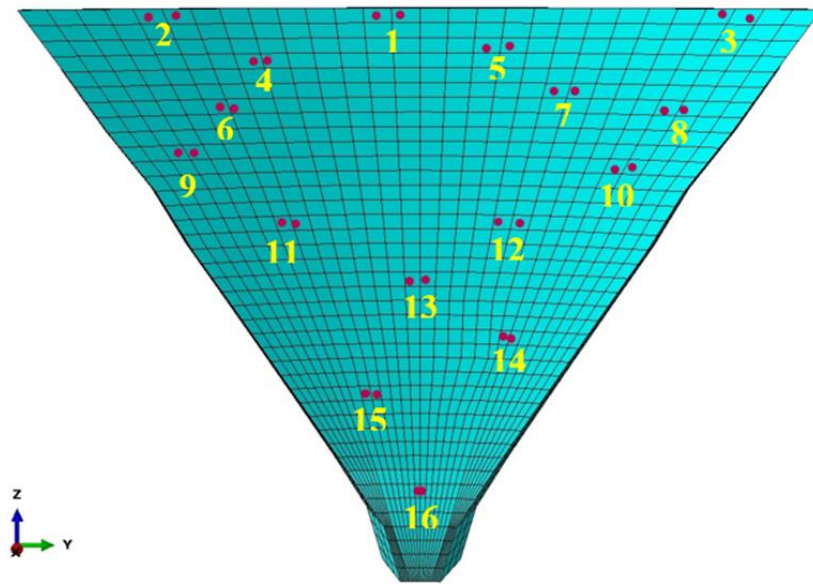


Fig.2 Different failure scenarios at different locations of the concrete arch dam

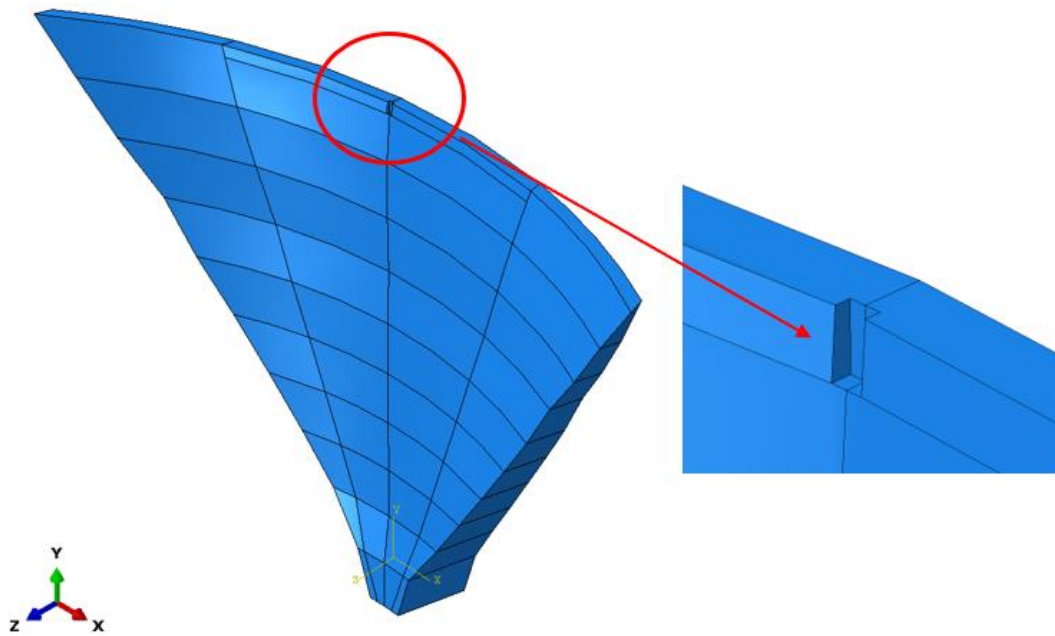


Fig.3 Created crack at point 1 for performing modal analysis

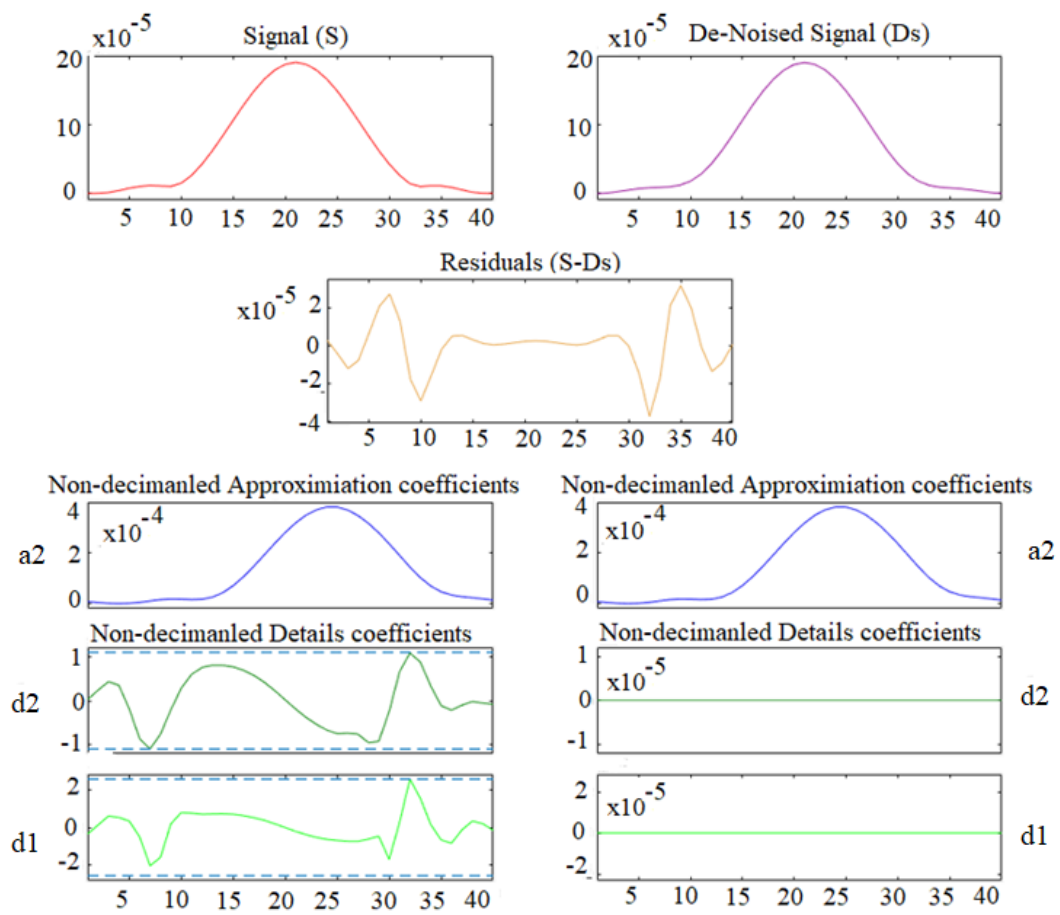


Fig.4 STW graph for the response of the healthy sample under the wavelet analyzer db2 (Model-U1)

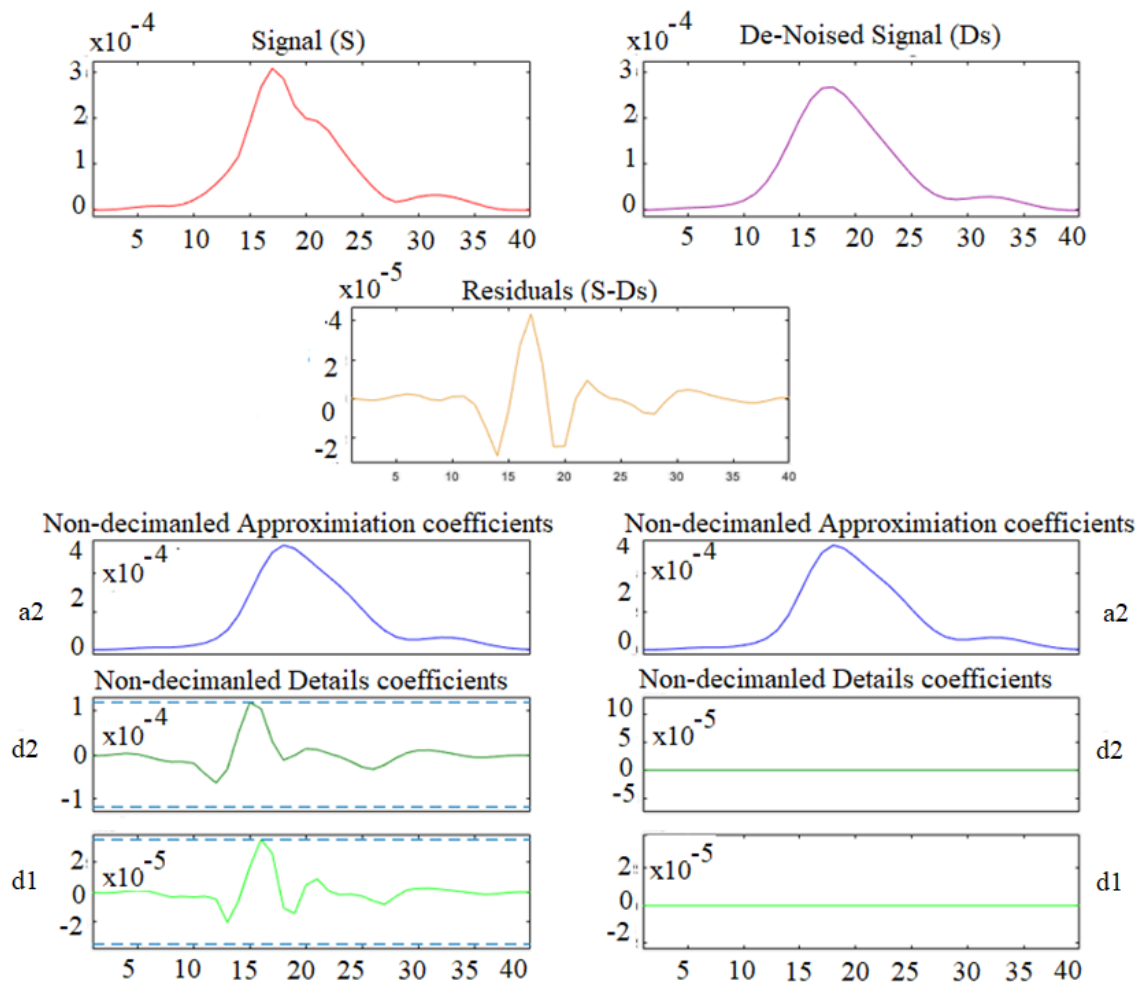


Fig.5 STW graph for the response of the cracked sample under the wavelet analyzer db2 (Model-U1)



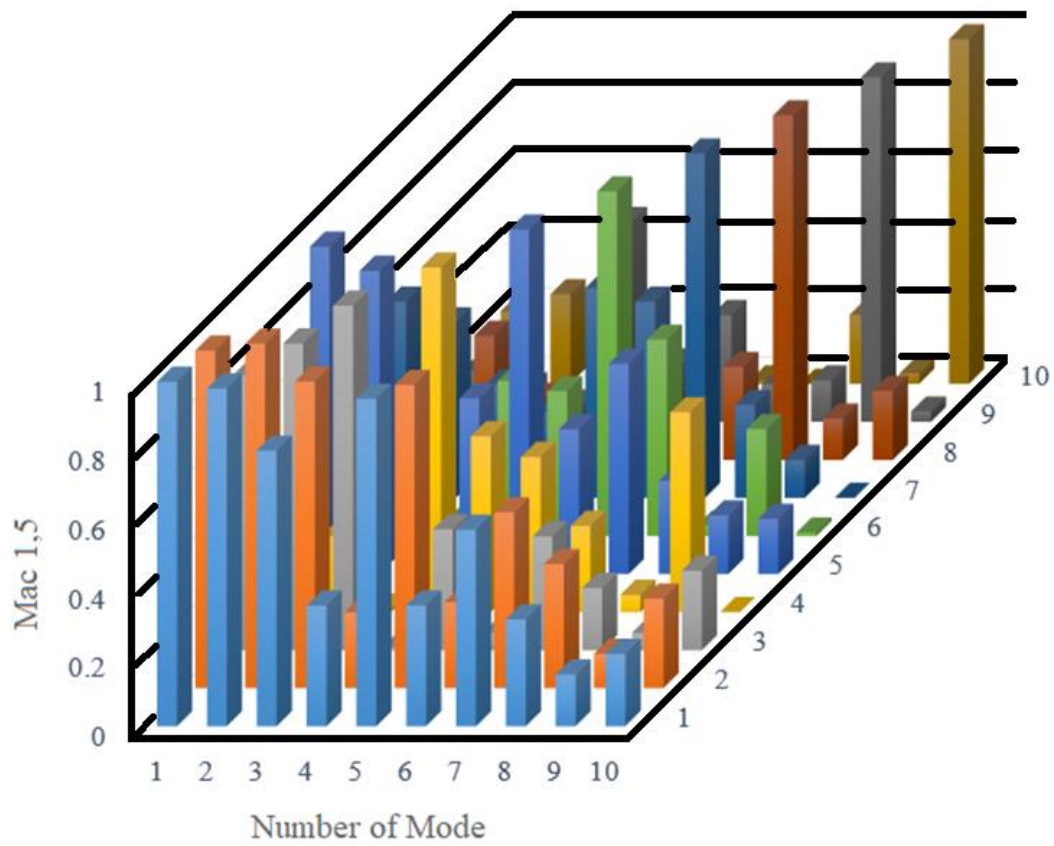


Fig.6 MAC matrix along Z axis for the first 10 modes of point 5

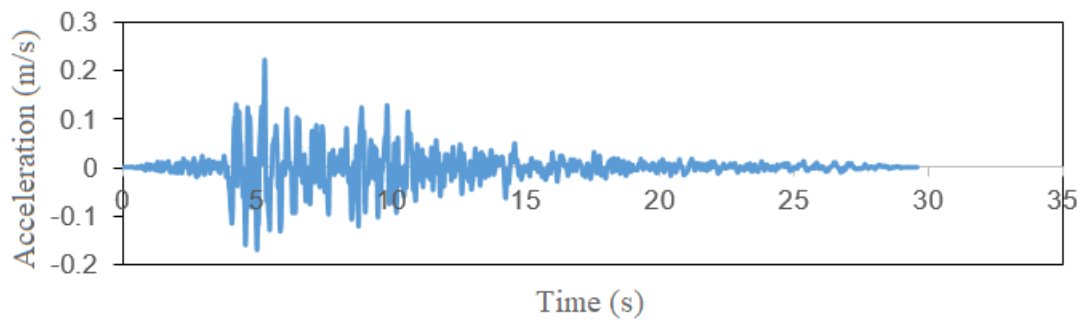


Fig.7 Accelerogram records of Northridge Earthquake

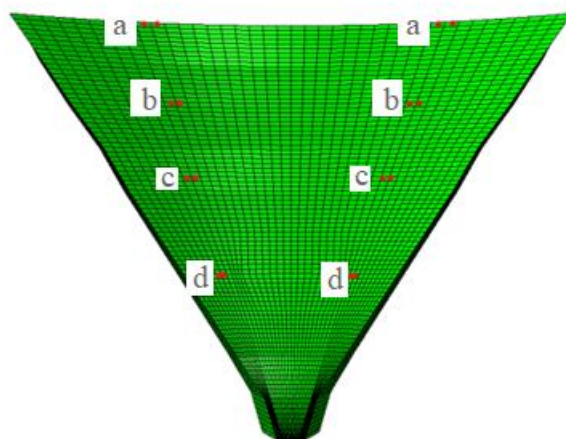


Fig.8 Selected points on the model of studied dam used for dynamic wavelet transform



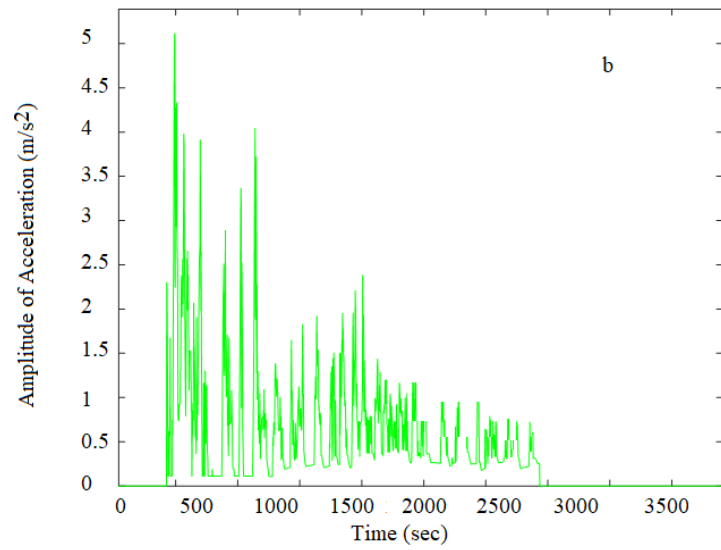
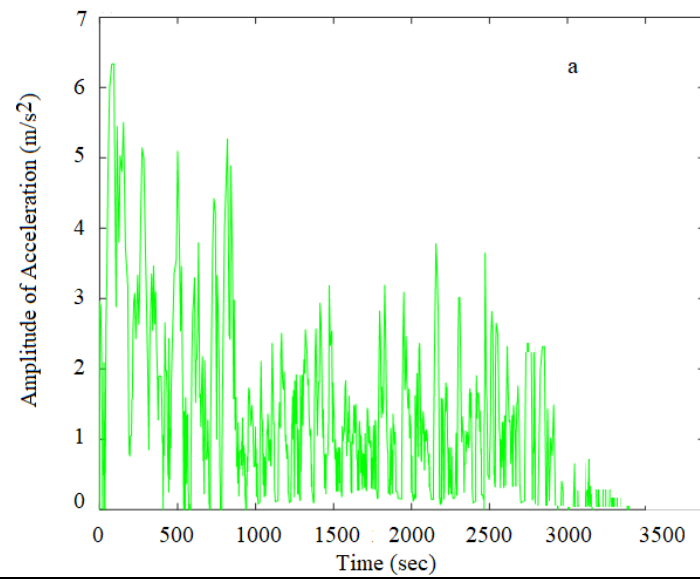
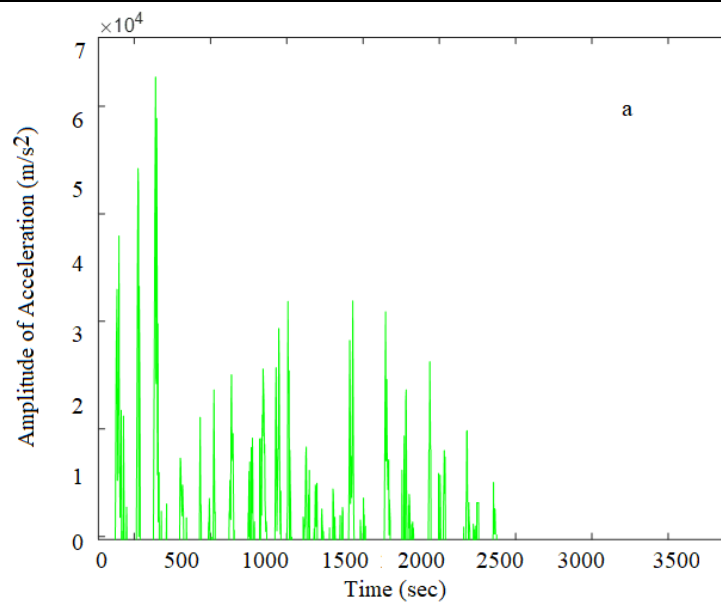


Fig.9 Difference between acceleration values corresponding to before and after 10% failure



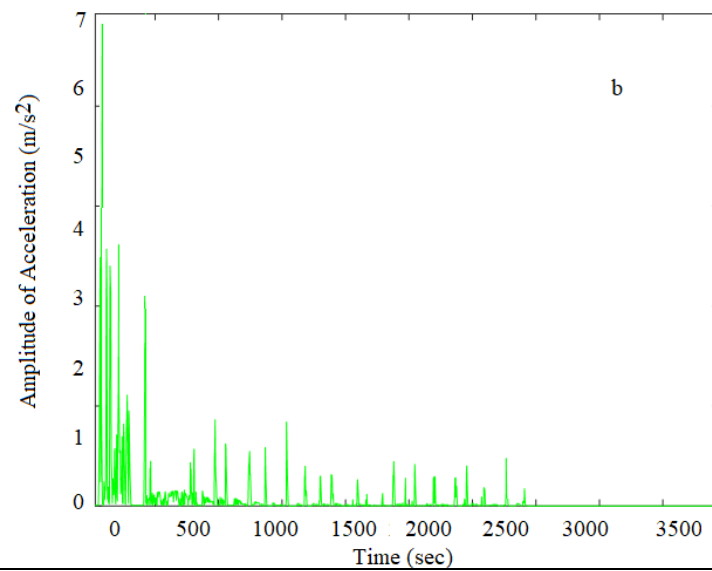


Fig.10 Difference between acceleration values corresponding to before and after 30% failure

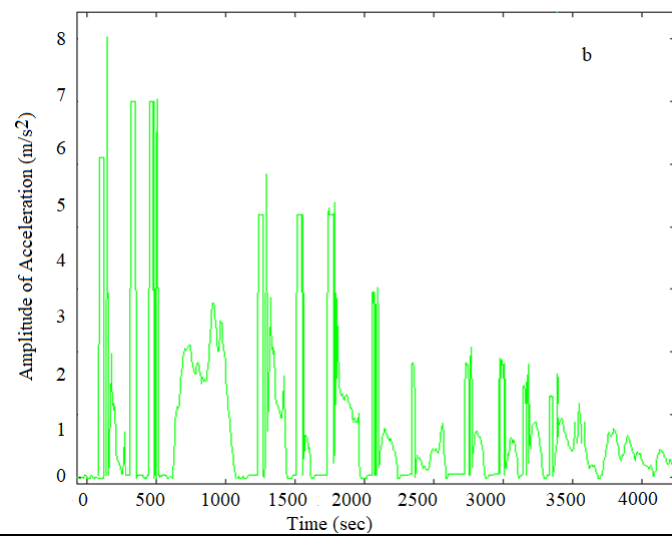
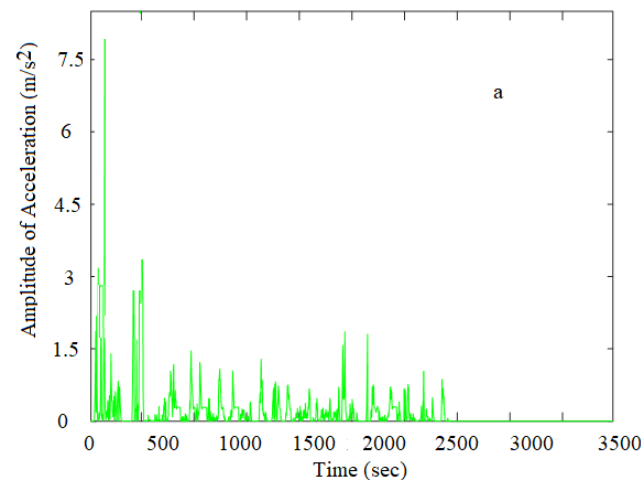


Fig.11 Difference between acceleration values corresponding to before and after 50% failure

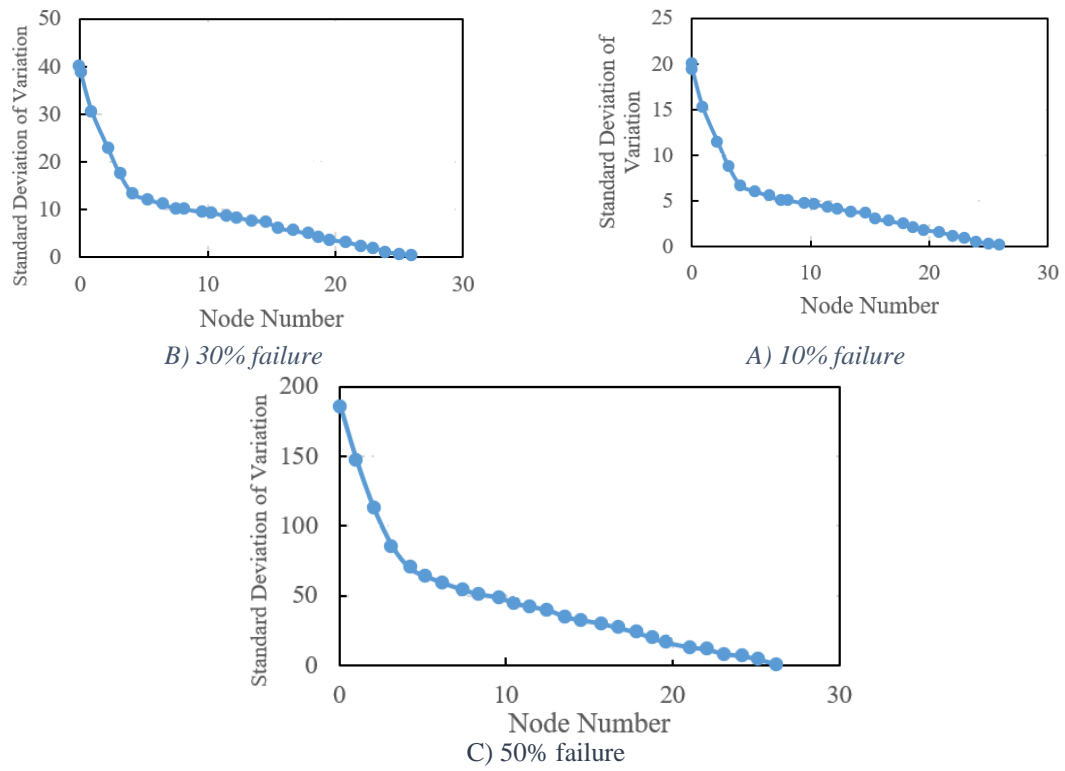


Fig.12 Standard deviation of acceleration changes corresponding to different structural nodes for 10, 30 and 50% failure rates.

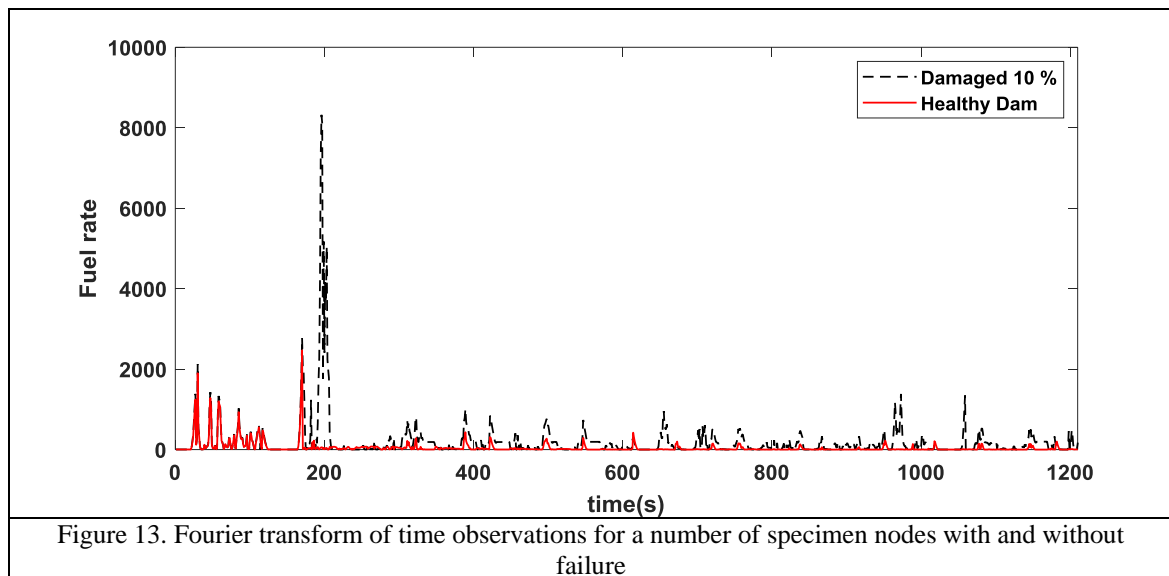


Figure 13. Fourier trnition of time observations for a number of specimen nodes with and without failure

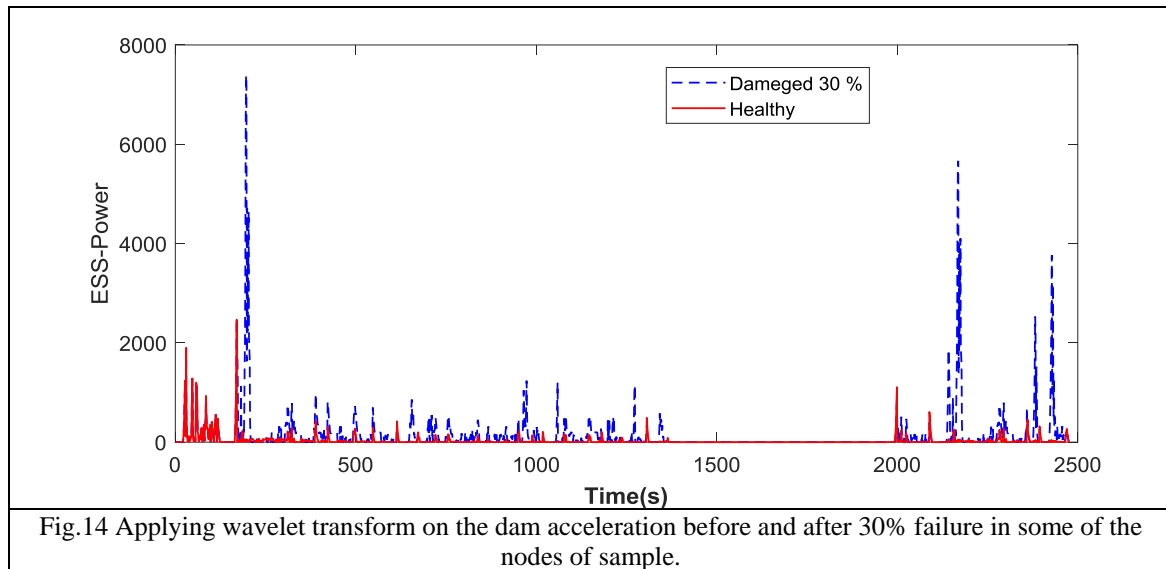


Table 1 Mechanical properties of the used materials in the dam

Unit	Value	Property
KN/m <sup>2</sup>	21	Specific weight
GPa	23.5	Modulus of elasticity
-	0.3	Poisson's ratio

Table 2 Properties of the dam and water behind the studied dam [30]

Modulus of elasticity	Poisson's ratio	Specific weight(kg/m <sup>3</sup> )	Type
27	0.2	2400	Concrete dam
25	0.167	0	Foundation
22	-	1000	Water

Table 3 Frequency modes of the studied dam

[30]	Presented study	Mode
1.52	1.42	1
1.54	1.43	2
2.05	2.08	3
2.27	2.36	4
2.53	2.63	5
2.94	2.99	6
3.19	3.25	7
3.32	3.28	8
3.72	3.68	9
3.90	3.99	10

Table 4 Location of the selected points

z	y	x	Number of point
2	220	-18	1
20.5	220	-91.68	2
25	220	100	3
10.8	195	-69	4
2.4	200	19.5	5
13.4	175	-67.5	6
8.5	185	50.5	7
14.9	178	70.6	8
16	155	-73.5	9
11.5	145	59	10
7.35	125	-42	11

5	125	31	12
2.3	75	0	13
4.4	65	26	14
3	45	-7	15
3.5	10	0	16

Table 5 The values of the first ten frequencies of the structure due to damage in different areas of the dam

Mo de	Frequencies of a healthy structure	Frequencies of damaged structures due to various damaged elements in the dam								
		Element 1			Element 2			Element 3		
		10%	30%	50%	10%	30%	50%	10%	30%	50%
1	1.42412	1.400 09	1.349 5	1.269 33	1.406 69	1.356 09	1.279 84	1.400 09	1.349 5	1.269 33
2	1.42868	1.408 64	1.370 58	1.312 66	1.408 12	1.363 68	1.303 58	1.408 64	1.370 58	1.312 66
3	2.08829	2.048 24	1.951 63	1.807 13	2.062 39	1.999 68	1.914 26	2.048 24	1.951 63	1.807 13
4	2.36354	2.343 38	2.302 4	2.214 73	2.329 77	2.242 47	2.112 58	2.343 38	2.302 4	2.214 73
5	2.63352	2.579 82	2.459 08	2.319 16	2.607 75	2.541 52	2.444 95	2.579 82	2.459 08	2.319 16
6	2.99817	2.961 06	2.883 37	2.746 91	2.964 44	2.883 94	2.774 7	2.961 06	2.883 37	2.746 91
7	3.26218	3.206 21	3.062 25	2.878 21	3.227 11	3.139 97	3.018 67	3.206 21	3.062 25	2.878 21
8	3.28758	3.259 66	3.226 21	3.176 01	3.255 63	3.178 75	3.067 19	3.259 66	3.226 21	3.176 01
9	3.68031	3.651 78	3.595 2	3.444 69	3.659 08	3.602 94	3.203 71	3.651 78	3.595 2	3.444 69
10	3.99447	3.915 39	3.732 04	3.515 47	3.951 65	3.786 92	3.460 38	3.915 39	3.732 04	3.515 47

Table 6. Changes in the natural frequencies due to presence of failure with different severities at the top of the concrete arch dam

	Percentage difference of Mode shapes															
	1	0.015	0.01	0.08	0.12	0.15	0.16	0.22	0.28	0.28	0.3	0.3	0.37	0.4	0.39	0.42
Number of Modes	1	0.015	0.01	0.08	0.12	0.15	0.16	0.22	0.28	0.28	0.3	0.3	0.37	0.4	0.39	0.42
	2	0.01	0.01	0.085	0.14	0.08	0.18	0.12	0.16	0.22	0.28	0.29	0.29	0.35	0.34	0.37
	3	0.02	0.015	0.025	0.09	0.05	0.1	0.08	0.1	0.32	0.26	0.28	0.44	0.5	0.5	0.47
	4	0.01	0.015	0.15	0.32	0.26	0.43	0.28	0.3	0.12	0.31	0.32	0.21	0.25	0.21	0.23
	5	0.022	0.015	0.02	0.08	0.05	0.09	0.05	0.08	0.33	0.24	0.26	0.38	0.44	0.51	0.52
	6	0.012	0.01	0.12	0.28	0.18	0.32	0.27	0.32	0.21	0.25	0.27	0.031	0.34	0.32	0.32
	7	0.02	0.01	0.11	0.22	0.12	0.38	0.22	0.28	0.28	0.26	0.27	0.38	0.43	0.46	0.42
	8	0.01	0.01	0.1	0.11	0.09	0.15	0.1	0.14	0.12	0.25	0.26	0.14	0.18	0.16	0.15
	9	0.008	0.006	0.25	0.26	1.3	0.42	0.29	0.31	0.28	0.38	0.18	0.25	0.22	0.2	0.18
	10	0.022	0.016	0.42	0.1	0.06	0.09	0.09	0.09	0.05	0.4	0.32	0.38	0.42	0.08	0.1

**Bio:**

Amir Meysam Giahi is a PhD Candidate in structural engineering. He now do researches in Department of civil, Faculty of technical engineering, Islamic Azad University, Central Tehran Branch, Tehran, Iran. His areas of expertise and research interests include Seismic strengthening, Optimization and structural health monitoring.

Dr. Jafar ASGARI Marnani is assistant Professor at Islamic Azad University, Central Tehran Branch, Technical Faculty, Civil Engineering Department. His research interests are Boundary Element Methods (BEM), Finite Element Methods (FEM), Numerical Methods in Engineering, Behavior of Steel Structures, Structural Optimization. He is working on the researches in the Non Linear Analysis of Continuum Media Using FEM - BEM.

Dr. Mohammad sadegh Rohanimanesh is assistant prof in Civil Engineering Group, Civil and Earth Resources Engineering Faculty, Central Tehran Branch, Islamic Azad University, Tehran, Iran. He has graduated of Ph.D. in 1995 from virjnia University, Department of earthquake. Research interests are Base isolation systems, seismic dampers, and seismic response of ratating systems.

Dr. Hassan Ahmadi is Assistant Prof. in Civil Engineering Group, Roudehen Branch, Islamic Azad University, Tehran, Iran. He has graduated of civil engineering in 2006 from Islamic Azad University, Science and Research Branch, Tehran, Department of civil engineering, and his research interests are Modeling and Simulation, Fluid Mechanics, Reservoir Engineering.